# RSC Advances

ROYAL SOCIETY OF CHEMISTRY

www.rsc.org/advances

# Probing the persistence of energy-level control effects at organic semiconductor/electrode interfaces based on photoemission spectroscopy combined with Ar gas cluster ion beam sputtering

Dong-Jin Yun*, Taeho Shin, SungJun Park, Youngsik Shin, YongKoo Kyung, JaeGwan Chung, and Yongsu Kim

Analytical Science Laboratory of Samsung Advanced Institute of Technology
Samsung Advanced Institute of Technology, Gyeonggi-do 443-803, Republic of Korea

* Corresponding author.

Tel: 82 3110 7471 3501; E-mail: Dongjin.yun@samsung.com

*1$^{st}$ revision submitted* to RSC advances

Aug. 28, 2015

## Abstract

Oxygen ($O_2$) plasma treatment is one of the most widely applied methods for modifying the electrode work function. However, owing to the instability of $O_2$-plasma treatment effects under air-exposed conditions, it is necessary to confirm whether the $O_2$-plasma treatment effects can be continuously maintained at organic semiconductor/electrode interfaces in realistic devices. In the present study, the electronic structures of organic semiconductor/$O_2$-plasma treated electrode interfaces were characterized by using *in situ* deposition and ultraviolet photoemission spectroscopy analysis. The structures of the corresponding samples were re-analyzed after a 1-week-long exposure to air to confirm the energy-level changes. To achieve this, we inceptively designed the studies of the energy level alignments of air-exposed samples based on the photoemission spectroscopy combined with Ar gas cluster ion beam sputtering process. The results of our studies clearly confirm the consistency of $O_2$-plasma treatment effects at organic semiconductor/electrode interfaces. In addition, we confirmed the preservation of controlled energy-level structures at $C_{60}$/Au interfaces by examining the relative rates of electron transfer at the $C_{60}$/Au interfaces, obtained from photoluminescence (PL) measurements.

## 1. Introduction

Compared to inorganic devices, organic devices are lightweight, bendable, cost efficient, and allow for low temperature processing.[1,2] Therefore, several research groups have conducted studies for enhancing the electrical performance/stability of real-life organic devices.[1-4] Despite the considerable progress achieved recently in improving the performance of organic devices, many design, material, and process parameters remain to be improved. In addition to the material properties of individual components, the contact resistances at organic semiconductor/electrode interfaces strongly affect the charge carrier motility in organic devices.[1,5,6] Therefore, optimization of the carrier injection barriers between organic semiconductor and electrode is one of the critical factors determining the electrical performance of an organic device.

Regarding the modification of the electrode-work function, the oxygen ($O_2$) plasma treatment has been one of the most widely applied methods.[7,8] In the $O_2$-plasma treatment process, the surface complex reactions accompany the surface contamination cleaning, partial oxidation and chemical/physical oxygen adsorption and as a result, the work functions of electrode surfaces increase.[7,8] In accordance with the purpose, this process has been consistently applied to a variety of metal/metal oxide/organic electrode materials, including gold (Au), indium tin oxide (ITO) and Poly(3,4-ethylenedioxythiophene):Polystyrene sulfonate (PEDOT:PSS).[7-9] Many studies demonstrated that the $O_2$-plasma treatment can effectively increase the electrode work function, adjusting the carrier injection barrier at organic semiconductor/electrode interfaces in various organic devices such as organic light emitting device (OLED), organic photovoltaic (OPV) and organic thin film transistor (OTFT).[1,7] However, to the best of our knowledge, only a few studies systematically examined the persistence of the $O_2$-plasma treatment effects.[10,11]

In this respect, our group operates one of the most advanced analytical facilities based on self-constructed photoemission spectroscopy system (PES), allowing the *in-situ* organic semiconductor growth and Ar gas cluster ion beam (Ar GCIB) sputtering as well as performing the ultraviolet photoelectron spectroscopy (UPS) /X-ray photoelectron spectroscopy (XPS) analyses.[12]

For this study, two sets of as-deposited and $O_2$-plasma treated Au and PEDOT:PSS films were prepared and fullerene ($C_{60}$) layers (thickness: ~ 15 nm) were grown on one of those sets. Then, all samples were stored in ambient air at 20 $^{o}$C and 50 %RH, and their chemical/energy level structures were periodically examined. After air-storage for 1 week, the carrier injection barriers of $C_{60}$/as-deposited and $C_{60}$/$O_2$-plasma treated Au structures were directly investigated by using the UPS analysis combined with Ar GCIB sputtering, respectively.

## 2. Experimental section

The $C_{60}$ (purity: 99.5 %) and PEDOT:PSS solution (Clevios$^{TM}$ PH 500) were purchased by Sigma-Aldrich and Heraeus both of them were used without any further purification process. The thermally grown $SiO_2$ (300 nm) on Si wafers were used as substrates due to smooth surface roughness (~0.2 nm) and insulating properties of $SiO_2$ layer. After the ultraviolet-ozone cleaning process (for 10 min. in air), the Au/Ti (50 nm/3 nm) and PEDOT:PSS (~ 50 nm) films were prepared by using thermal evaporation (at room temperature and $10^{-6}$ Torr) and spin-coating (5000 rpm)/annealing (150 $^{o}$C in air) processes, respectively. The $O_2$-plasma treatment (RF power: 50 W) was conducted in the vacuum chamber (Covance-1MP produced by FEMTO science) for 5 min. under $O_2$ gas (purity: 99.9 %) flow conditions (at room temperature and $10^{-1}$ Torr). Subsequently, $O_2$-plasma treated Au and PEDOT:PSS films were transferred to self-constructed PES system, which unfortunately exposed the samples to air for ~ 1 min.. The $C_{60}$ layers (thickness: ~ 15 nm) were deposited by thermal evaporation process in preparation UHV chamber (at room temperature and $10^{-8}$ Torr).[12] Simultaneously, using monochromatic He II source and electron analyzer system, the UPS spectra were obtained for characterizing the energy level alignments of $C_{60}$/electrode (Au and PEDOT:PSS) structures.[12]

After air-storage for 1 week, the samples are put into a commercial PES instrument (VersaProbe PHI 5000, manufactured by ULVAC-PHI). The *in-situ* valence band and core-level analyses were performed by using the UPS (He I source)/XPS (monochromatic AlKα source) photoemission spectroscopy in conjunction with Ar GCIB sputtering process. A 10 × 10 mm$^2$ raster and an acceleration voltage of 10 kV were chosen as the default settings for the Ar GCIB sputtering process. The base pressure of UHV chamber was maintained at $10^{-6}$ Torr during the XPS (beam diameter: 100 um)/UPS (beam diameter: ~5 mm) measurements. Photoluminescence (PL) measurements were performed by using a picosecond laser (Picoquant) with a wavelength of 405 nm and a charge-coupled device detector that was cooled to 200 K. The wavelength of 405 nm was used because of its suitable domain for create electron-hole pair in C60 molecule and reference PL signal from Au substrate.

## 3. Results and discussion

The schematic diagram in Figure 1 (a) summarizes the experiment for studying the persistence of the $O_2$-plasma treatment effects on the energy level alignments at organic semiconductor/electrode interface. To ensure the experimental accuracy, at the same time, the energy level alignments of as-deposited and $O_2$-plasma treated electrodes were immediately investigated before and after the *in-situ* $C_{60}$ growth process. Throughout this process, the energy band diagrams of $C_{60}$/electrode structures were constructed and are shown in Figures 1 (b) and (c). Then, with reference to these energy band diagrams, the energy level changes were monitored at regular intervals throughout the entire period of exposure to ambient air. Various kinds of electrode materials such as Ag and ITO are widely used as electrodes of organic/inorganic devices. Among them, the Au electrode has been particularly used as a reference electrode in organic thin film transistor due to high work function. Besides, we believe that the excellent air-stability of Au film leads to the fast recovery to its original state from the newly formed state by $O_2$ plasma treatment. That is why the Au electrode was mainly investigated for the air-aging properties of the controlled energy level with or without $C_{60}$ deposition.

Figures 1 (b) and (c) show the energy band level alignments at $C_{60}$/as-deposited Au and $C_{60}$/$O_2$-plasma treated Au structures, respectively. The band gap energy ($E_g$ = 2.30 eV) of $C_{60}$ was obtained from previous report, which reveals the actual transport gap between the highest occupied molecular orbital (HOMO) and the lowest unoccupied molecular orbital (LUMO) levels in the UPS-Inverse photoemission spectroscopy (IPES) spectra of $C_{60}$ film.[12,13] As summarized in Figures 1 (b) and (c), the $O_2$-plasma treatment increased the Au work function from 5.04 eV to 5.71 eV; subsequently, this work function change resulted in distinctive energy level alignment.[7,14,15] Owing to the high work function of $O_2$-plasma treated Au electrode, the *in-situ* grown $C_{60}$ (~15 nm) on as-deposited Au electrode develops higher hole-injection barrier ($\Phi_H$: 1.39 eV) than that ($\Phi_H$: 0.97 eV) of as-deposited Au electrode.

As shown in Figures 2 (a)-(d), the comparative UPS spectra of $C_{60}$/Au ((a) secondary cutoff region and (b) valence band structure) and $C_{60}$/PEDOT:PSS structures ((c) secondary cutoff region and (d) valence band structure) were characterized during *in-situ* growth/analysis process. Both $O_2$-plasma treated Au (5.71 eV) and PEDOT:PSS (5.52 eV) films exhibited relatively higher work functions than those of the corresponding as-deposited ones (5.04 eV for Au and 5.18 eV for PEDOT:PSS) to varying extents. As a result, the $\Phi_H$ values of these $C_{60}$/$O_2$-plasma treated electrode interfaces decreased, even allowing for the vacuum level shift induced by the interfacial dipoles. The results clearly indicate that $O_2$-plasma treatment allows controlling the energy level alignments at organic semiconductor/electrode interfaces.[14,15] To study the persistence of these effects, the electronic structure variations of electrode and $C_{60}$/electrode were consistently monitored at different time points during the exposure to ambient air.

Figures 3 (a) and (b) involve the comparative XPS core level structures, revealing the variations in the chemical states of $O_2$-plasma treated Au and PE under air-storage conditions. After the $O_2$-plasma treatment, the Au-$O_x$ chemical state newly emerges at Au surface and the ratio of carbon-oxygen (-COOH and -COH) to carbon-carbon bonds (C=C and C-C) significantly increases at the PE surface, respectively. During air-storage, newly formed carbon-oxygen bonds in PEDOT:PSS are partially retained whereas the chemical state of Au completely returns to the inherent Au metallic state. However, despite of such difference, air-storage usually increased the relative carbon/oxygen percentage in Au and PEDOT:PSS films, as shown in Figures 3 (c) and (d).

The $O_2$-plasma treatments resulted in the valence band changes owing to the reactions of surface components with highly activated oxygen species.[16] Therefore, as-deposited and $O_2$-plasma treated electrodes exhibited strong differences in electronic configurations of Au (C 2p, O 2p and Au 5d hybrid orbitals) and PEDOT:PSS (C 2p, O 2p and S 3p).[17,18] On the other hand, along with the chemical states and the atomic composition, the electronic structures of the $O_2$-plasma treated electrodes changed significantly during the air-storage. Figures 4 (a) and (b) show the variations of electronic structures in Au and PEDOT:PSS UPS spectra with duration of air exposure. Interestingly, the valence band structures of $O_2$-plasma treated Au and PEDOT:PSS gradually became similar to those of the corresponding as-deposited ones at increasing exposure times. Moreover, in accordance with those transitions, the same variation trends were observed in the Au and PEDOT:PSS energy level structures. Figure 4 (c) shows that, during air-storage, the elevated work functions arising from $O_2$-plasma treatments gradually dropped according to the exposure time to ambient air; eventually, the work function differences between as-deposited and $O_2$-plasma treated structures became imperceptible after 2 days of exposure. The PES studies on chemical/electronic structures obviously verified that the oxide layers or partially oxidized functional groups, induced by $O_2$-plasma treatment, are not fully stabilized and remain significantly reactive owing to high surface energy.[7,14,19-21] In other words, the newly formed energy level structures at the surface could not be maintained under exposure to air.[22] Furthermore, as the UPS spectra in Figure 4 (d) show, the $C_{60}$/Au exposed to ambient air for 1 week almost lost their inherent electronic configurations, precluding the accurate analysis of the energy level alignments at the corresponding interface.[22] Thus, the controlled energy level alignment at organic semiconductor/electrode interface could not be continuously preserved with certainty. Thereby, it is necessary to clarify whether the energy-level control effects persist under working conditions. In this respect, the PES combined with Ar GCIB sputtering process can be a unique method for directly testing this issue.[12]

Through exhaustive studies based on various organic materials including layered, blended and composite structures, our group has obtained strong evidence that the Ar GCIB sputtering insignificantly affects the chemical/electronic structures in the UPS/XPS spectra of organic-based materials.[12] Thereby, this allows using the PES analysis for determining accurate energy level alignments corresponding to the depth position from air-exposed surface to the bulk. As shown in Figures 5 (a)-(d), the electronic structures of $C_{60}$ films remain intact under oxidized surface layers. The valence band structures also maintain unchanged energy-level alignments at their corresponding $C_{60}$/Au interfaces. Besides, the secondary cutoff regions of UPS spectra include the controlled work function (5.8 eV) at the surface of $O_2$-plasma treated Au electrode.

As shown in Figures 6 (a) and (b), comparative UPS spectra yield the energy level alignments at the $C_{60}$/Au interface below the air-exposed surface. These results clearly demonstrate that, after 1 week of air-storage, the $C_{60}$/Au interface still retains its inherent electronic configuration and energy level alignments. The $\Phi_H$ ($C_{60}$/as-deposited Au: 1.41 eV and $C_{60}$/$O_2$-plasma treated Au: 1.06 eV) of air-exposed $C_{60}$/Au, for example, is approximately equal to that of the corresponding one ($C_{60}$/as-deposited Au: 1.39 eV and $C_{60}$/$O_2$-plasma treated Au: 0.97 eV). Thereby, the carrier injection barriers of $C_{60}$/$O_2$-plasma treated Au still retain energy gaps of ~ 0.35 eV compared with those of $C_{60}$/as-deposited Au. Besides, the work functions at different depth positions definitely reflect the work function difference between as-deposited and $O_2$-plasma treated one. In addition, in contrast to $C_{60}$/as-deposited Au, the $C_{60}$/$O_2$ plasma Au has another chemical state as well as Au metal state in the Au 4f core level structure of Figure 5 (d). This small peak at 84.8 eV corresponds to Au-O partial oxidation state and confirms that the Au-O oxidation state still remains partially even after 1 week of exposure to air.[23] The comparative core-levels of $C_{60}$/Au in Figure 5 (d) completely supports the persistence of the elevated work function in $O_2$-plasma treated Au.

Through data integration of the UPS depth profiles, the energy level alignments at the interfaces of air-exposed C60/Au structures are summarized as energy band diagrams in Figure 7. During Ar GCIB sputtering, the morphological changes and the Au surface cleaning lead to certain numerical differences between vacuum-level shift and work function, respectively.[24] However, considering these experimental errors, the carrier injection barriers at the interface do not change significantly in spite of a 1-week-long air exposure. We believe that the controlled energy level alignments at the surface of $O_2$-plasma treated Au could be preserved by $C_{60}$ film serving as a passivation layer.

In addition, we demonstrated the preservation of controlled energy-level structure at the $C_{60}$/Au interface based on photoluminescence (PL) measurements, which allow examining the relative rates of electron transfer at the $C_{60}$/Au interface. Electron-hole pairs of photo-excited $C_{60}$ molecules undergo radiative- and non-radiative recombination processes.[25] However, the presence of contacting Au electrodes offers another channel for electron transfer from the Au electrode to $C_{60}$ molecules at the interface, consequently suppressing the photoluminescence from photo-excited $C_{60}$ molecules. The electron transfer rate is influenced by the reorganization energy (λ) and the free energy change (ΔG) before and after the electron transfer. Both of them determine the activation energy ($\Delta G^{\#}$) of the reaction across parabolic potential energy surfaces, and the rate is described as follows by the Marcus theory[26]

$$\gamma_{ET} \sim \exp(-\Delta G^{\#}) = \exp(-(\lambda + \Delta G)^2/4\lambda k_B T) \quad (1)$$

Figure 8 (a) shows the PL spectra from the as-prepared $C_{60}$/Au structures after optical excitation at 405 nm. The peak wavelength near 750 nm is in a good agreement with previous observations.[25] The $C_{60}$ films on as-deposited and $O_2$-plasma treated Au electrodes exhibit distinctive PL spectra. Despite the same thicknesses (~ 15 nm) of the samples, the PL intensity from the $C_{60}$ layer on the $O_2$-plasma treated Au electrode is appreciably higher (the relative ratio is ~ 1.7). This result can be explained by the electron transfer rate owing to the free energy change ($\Phi_e$ change in energy band diagram) described by Eq. (1). Because the work function of the Au electrode is increased by the $O_2$-plasma treatment, the free energy gain becomes smaller by 0.42 eV

(= 1.39 eV - 0.97 eV). This leads to a larger $\Delta G^{\#}$ for electron transfer and less efficient electron transfer between $C_{60}$ films and the $O_2$-plasma treated Au electrode. Accordingly, such a change increases the probability of radiative recombination, enhancing the photoluminescence intensity. Figure 8 (b) shows the change in the PL spectra of the same samples after 1 week of exposure to air. Compared to the PL spectra of the as-prepared sample, the relative intensity of the PL spectra changes negligibly within the period (the relative ratio is ~ 1.6) indicating that the $C_{60}$ layer prevents the transition of controlled energy level alignments from reduction of the $O_2$-plasma treated electrode by air. This result is consistent with the preservation of energy level alignments revealed by the earlier PES analysis.

## 4. Conclusions

In conclusion, the cyclic PES analysis for $O_2$-plasma treated electrodes reveals the instability of $O_2$-plasma treatment effects with exposure to air. Hence, it is necessary to confirm whether the $O_2$-plasma treatment effects can be maintained at organic semiconductor/electrode interfaces in real devices. To achieve this, we designed the PES-based method, which allows for direct characterization of the energy level alignments of air-exposed samples. The actual results clearly verify the persistence of energy-level control effects at organic semiconductor/electrode interfaces in various organic devices.

## Acknowledgments

## References

1. S. W. Rhee and D. J. Yun, *J. Mater. Chem.*, 2008, **18**, 5437.

2. D. J. Yun, S. H. Lee, T. W. Lee and S. W. Rhee, *Org. Electron.*, 2009, **10**, 970.

3. C. Reese, M. Roberts, M. Li and Z. Bao, *Mater. Today*, 2004, **7**, 20.

4. O. Knopfmacher, M. Hammock, A. Appleton, G. Schwartz, J. Mei, T. Lei, J. Pei and Z. Bao, *Nat. Comm.*, 2013, **5**, 2954.

5. D. J. Yun, S. H. Lee, K. Yong and S. W. Rhee, *Appl. Phys. Lett.*, 2010, **97**, 073303.

6. D. J. Yun and S. W. Rhee, *ACS Appl. Mater. Interfaces*, 2012, **4**, 982.

7. W. K. Kim, K. Hong and J. L. Lee, *Appl. Phys. Lett.*, 2006, **89**, 142117.

8. Y. Zhou, Y. Yuan, J. Lian, J. Zhang, H. Pang, L. Cao and X. Zhou, *Chem. Phys. Lett.*, 2006, **427**, 394.

9. K. Sugiyama, H. Ishii, Y. Ouchi and K. Seki, *J. Appl. Phys.*, 2000, **87**, 295.

10. Y. C. Chao, Y. C. Lin, M. Z. Dai, H. W. Zan and H. F. Meng, *Appl. Phys. Lett.*, 2009, **95**, 203305.

11. A. Sharma, B. Kippelen, P. J. Hotchkiss and S. R. Marder, *Appl. Phys. Lett.*, 2008, **93**, 163308.

12. D. J. Yun, J. Chung, Y. Kim, S. H. Park, S. H. Kim and S. Heo, *J. Appl. Phys.*, 2014, **116**, 153702.

13. M. S. Golden, M. Knupfer, J. Fink, J. F. Armbruster, T. R. Cummins, H. A. Romberg, M. Roth, M. Sing, M. Schmidt and E. Sohmen, *J. Phys. Condens. Matter.*, 1995, **7**, 8219.

14. W. Kim and J. L. Lee, *Electrochem. Solid-State Lett.*, 2007, **10**, H104.

15. S. Y. Kim, K. Hong, K. Kim, H. K. Yu, W. K. Kim and J. L. Lee, *J. Appl. Phys.*, 2008, 103, 076101.

16. A. Wolkenhauer, G. Avramidis, E. Hauswald, H. Militz, W. Viol, *Int. J. Adhes. Adhes.*, 2009, **29**, 167.

17. H. Shi, R. Asahi and C. Stampfl, *Phys. Rev. B.*,2007, **75**, 205125.

18. D. J. Yun, H. Ra, J. Kim, I Hwang, J. Lee, S. W. Rhee and J. Chung, *ECS. J. Solid State SC.*, 2012, **1**, M10.

19. L. K. Ono and B. R. Cuenya, *J. Phys. Chem. C*, 2008, **112**, 4676.

20. Z. Chen, M. Lee, R. S. Ashraf, Y. Gu, S. A. Seifried, M. M. Nielsen, B. Schroeder, T. D. Anthopoulos, M. Heeney, I. McCulloch and H. Sirringhaus, *Adv. Mater.*, 2012, **24**, 647.

21. A. Sharma, P. J. Hotchkiss, S. R. Marder and B. Kippelen, *J. Appl. Phys.*, 2009, **105**, 084507.

23. F. Ying, S. Wang, C. T. Au and S. Y. Lai, *Gold Bull.*, 2010, **43**, 241.

24. D. J. Yun, J. Chung, C. Jung, K. H. Kim, W. Baek, H. Han, B. Anass, G. S. Park and S. H. Park, *J. Appl. Phys.*, 2013, **114**, 013703.

25. Y. J. Lee, N. W. Song and S. K. Kim, *J. Phys. Chem. A*, 2002, **106**, 5582.

26. R. A. Marcus, *J. Chem. Phys.*, 1956, **24**, 966.

## Figure Captions

**Figure 1** (a) Schematic of the experimental concept for verifying the persistence of $O_2$plasma treatment effects on the energy level alignments at organic semiconductor/electrode interfaces and the energy band level alignments ((b) as-prepared $C_{60}$/as-deposited Au and (c) $C_{60}$/$O_2$-plasma treated Au structures) obtained by this experimental method.

**Figure 2** The comparative UPS spectra of $C_{60}$/Au ((a) secondary cutoff region and (b) valence band structure) and $C_{60}$/PEDOT:PSS structures ((c) secondary cutoff region and (d) valence band structure) characterized during *in-situ* growth/analysis process.

**Figure 3** The comparative XPS core levels yielding the chemical state changes of $O_2$-plasma treated (a) Au and (b) PEDOT:PSS during 1-week-long exposure to air, and the atomic concentrations ((c)) Au and (d) PEDOT:PSS) obtained based on them.

**Figure 4** The UPS spectra ((a) Au, (b) PEDOT:PSS and (d) C60/electrode) including the information about the configuration variations in valence band structures according to the exposure time to ambient air and (c) the variations of electrode work functions during 1-week-long exposure to air.

**Figure 5** The focused valence band regions ((a) $C_{60}$/as-deposited and (b) C60/$O_2$-plasma treated Au) and secondary cutoff regions ((a) $C_{60}$/as-deposited and (b) $C_{60}$/$O_2$-plasma treated Au) in the UPS depth profiles for the $C_{60}$/Au structures exposed to air for 1 week.

**Figure 6** The UPS spectra ((a) Au, (b) PE and (d) $C_{60}$/electrode) including the information about the configuration variations in valence band structures according to the exposure time to ambient air and (c) the variations of electrode work functions during 1-week-long exposure to air.

**Figure 7** The energy band level alignments of (b) $C_{60}$/as-deposited Au and (c) $C_{60}$/$O_2$-plasma treated Au structures, during 1-week-long exposure to air.

**Figure 8** Photoluminescence (PL) spectra of $C_{60}$/as-deposited Au (red line) and $C_{60}$/$O_2$-plasma treated Au structures (blue line). The PL spectra were obtained from as-prepared samples (a) and from samples that were exposed to air for 1 week (b). The PL spectra (black line) peaking near 540 nm were obtained from Au/$SiO_2$ samples for reference.

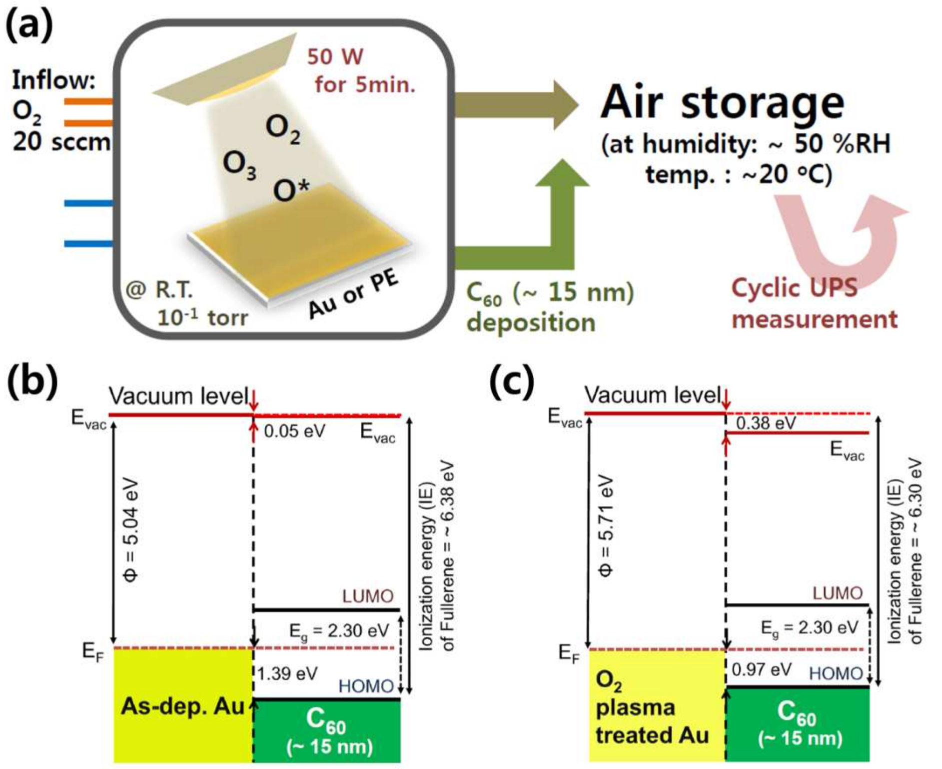

**Figure 1 Yun et al.**

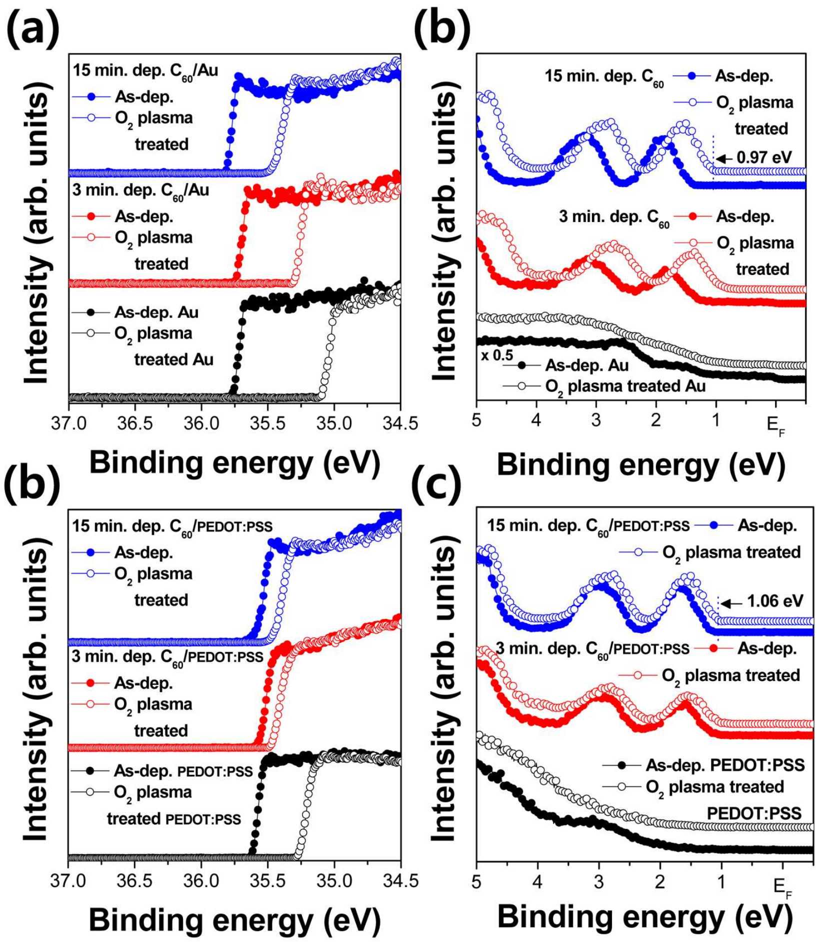

**Figure 2 Yun et al.**

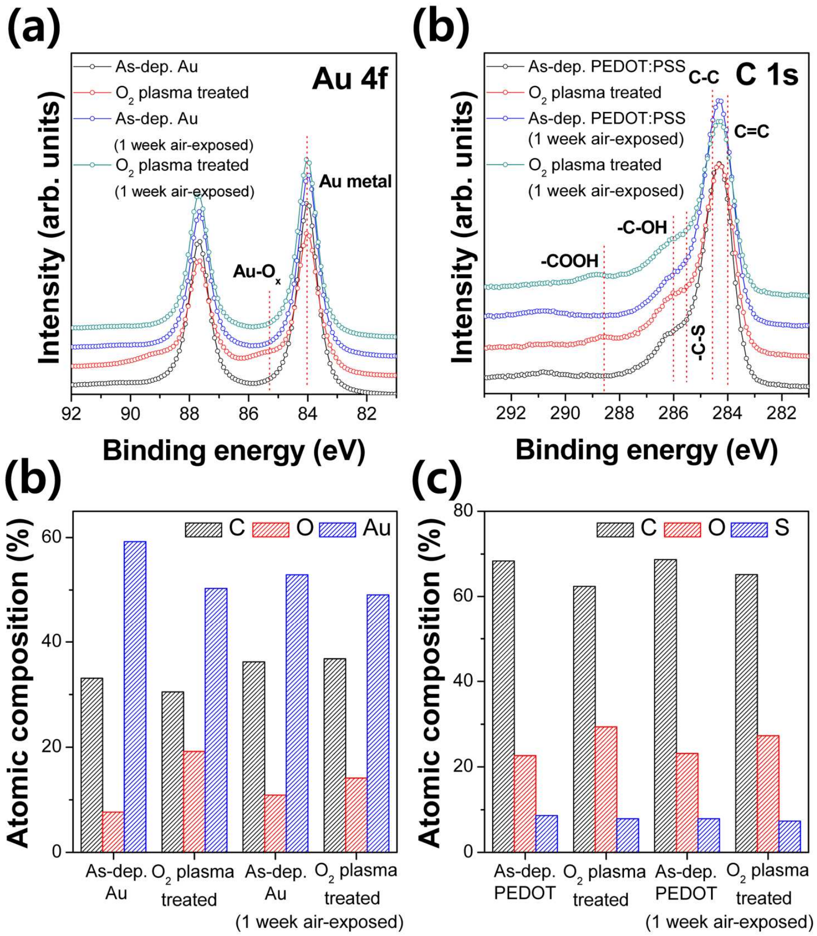

**Figure 3 Yun et al.**

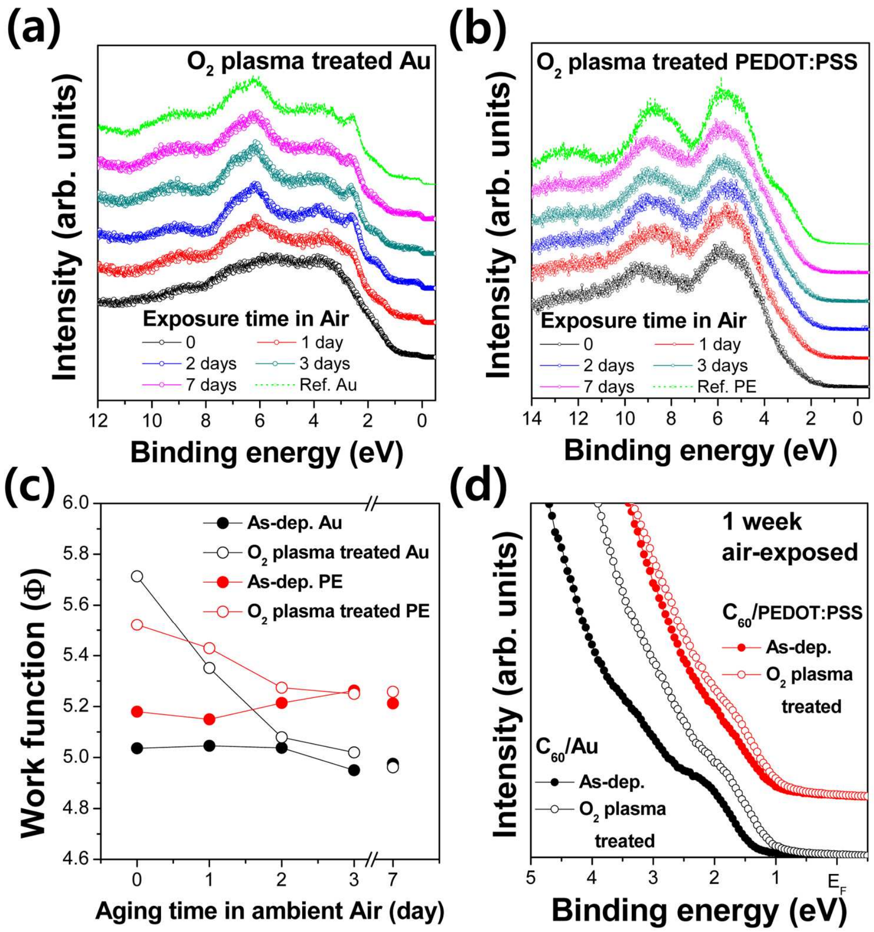

Figure 4 Yun et al.

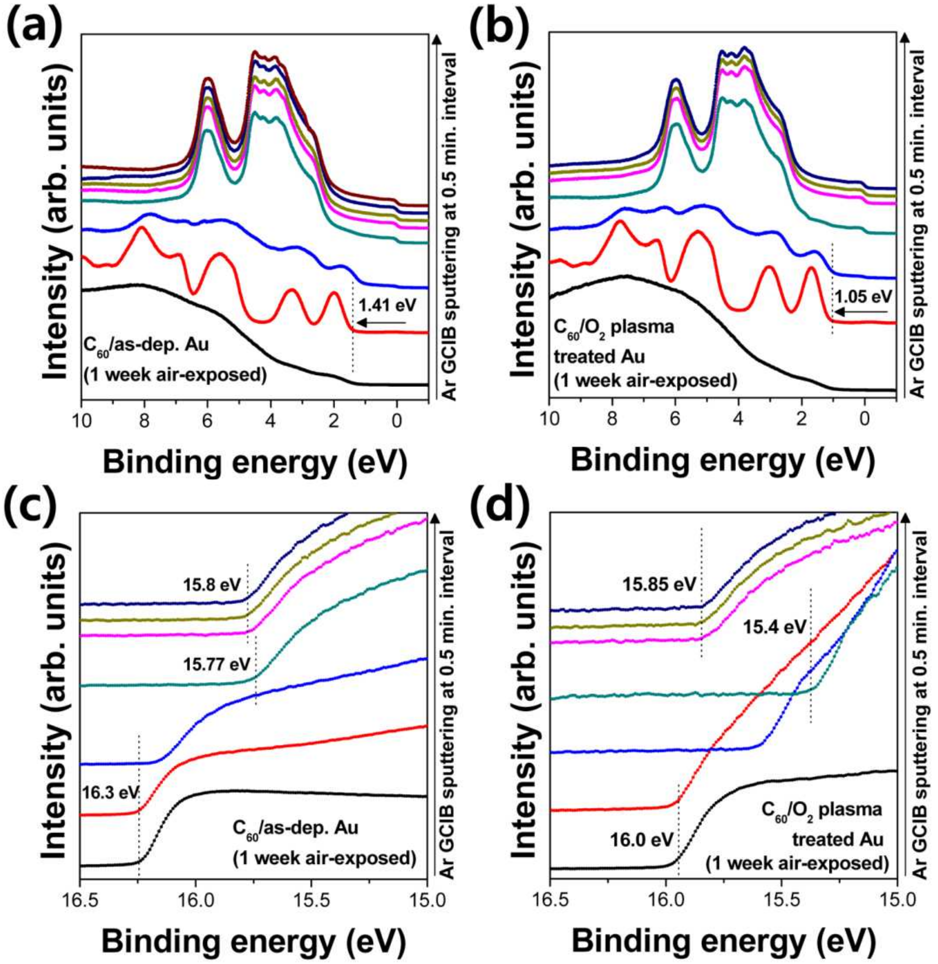

**Figure 5 Yun et al.**

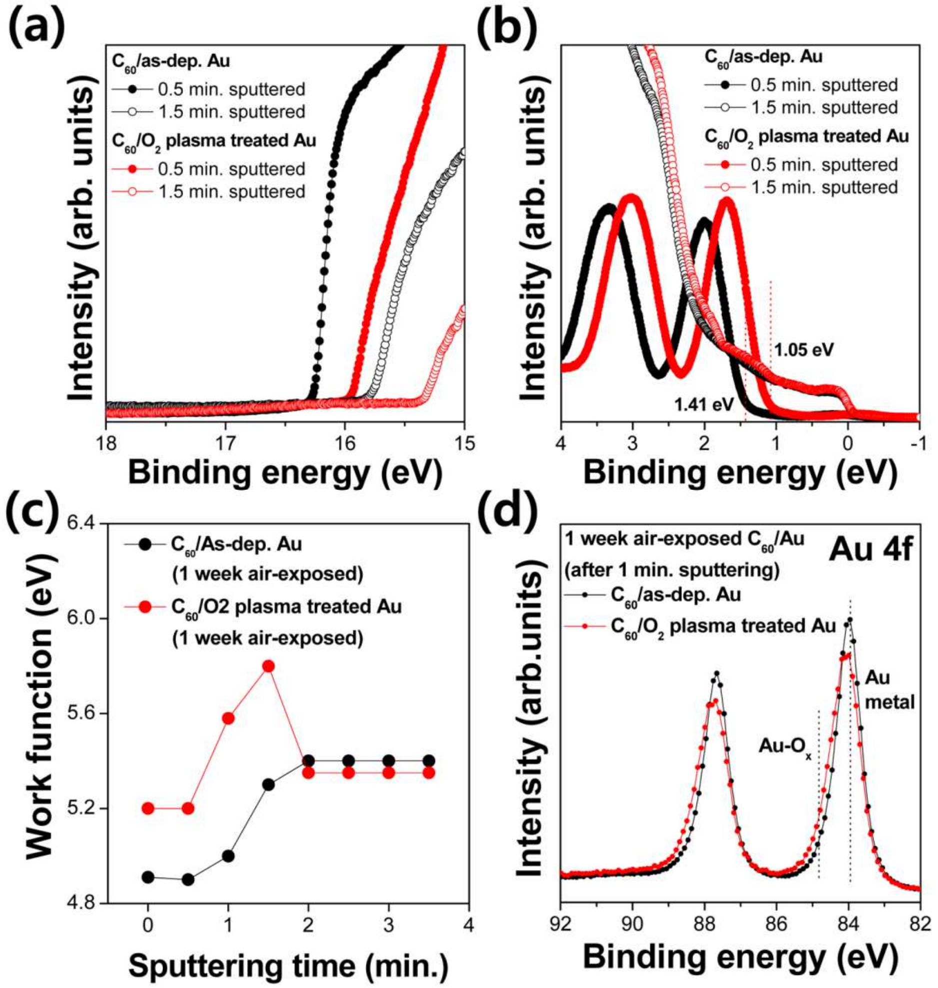

Figure 6 Yun et al.

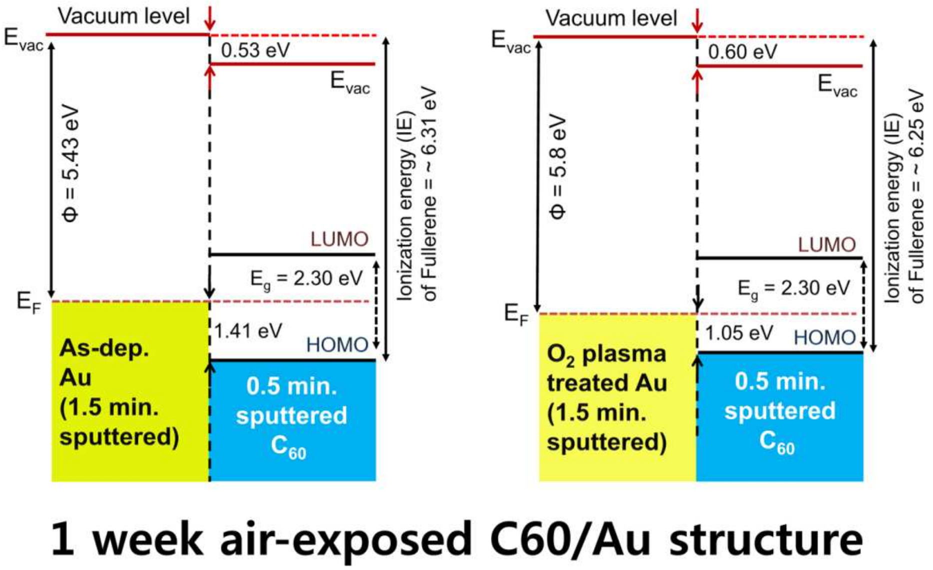

**Figure 7 Yun et al.**

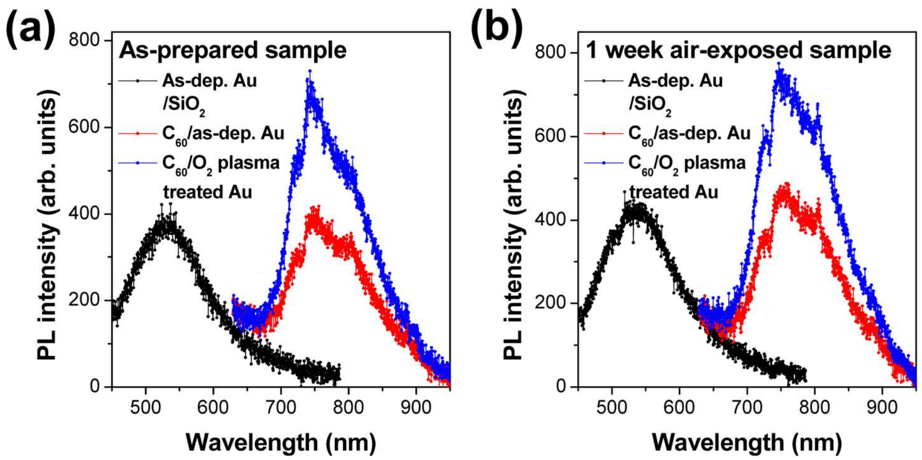

**Figure 8 Yun et al.**

The *in-situ* PES – Ar GCIB sputtering combined analysis enable to characterize the persistence of controlled energy-level at organic semiconductor/electrode interfaces